



Contents lists available at ScienceDirect

Dendrochronologia

journal homepage: [www.elsevier.com/locate/dendro](http://www.elsevier.com/locate/dendro)



## Application of eco-physiological models to the climatic interpretation of $\delta^{13}\text{C}$ and $\delta^{18}\text{O}$ measured in Siberian larch tree-rings

Olga V. Churakova (Sidorova)<sup>a,b,g,\*</sup>, Aleksandr V. Shashkin<sup>c</sup>, Rolf T.W. Siegwolf<sup>g</sup>, Renato Spahni<sup>h</sup>, Thomas Launois<sup>e,f</sup>, Matthias Saurer<sup>g</sup>, Marina V. Bryukhanova<sup>c,d</sup>, Anna V. Benkova<sup>c</sup>, Anna V. Kuptsova<sup>c</sup>, Philippe Peylin<sup>f</sup>, Eugene A. Vaganov<sup>c,d</sup>, Valerie Masson-Delmotte<sup>f</sup>, John Roden<sup>i</sup>

<sup>a</sup> University of Bern, Institute of Geological Sciences, Dendrolab.ch, 3012 Bern, Switzerland

<sup>b</sup> ETH Zurich, Department of Environmental Sciences, 8092 Zurich, Switzerland

<sup>c</sup> V.N Sukachev Institute of Forest SB RAS, 660036 Krasnoyarsk, Russia

<sup>d</sup> Siberian Federal University, 660041 Krasnoyarsk, Russia

<sup>e</sup> INRA, UMR 1391 ISPA, 33140 Villenave d'Ornon, France

<sup>f</sup> CEA Saclay—Laboratoire des Sciences du Climat et de l'Environnement, CEA Saclay, 91 191 Gif-sur-Yvette, Cédex, France

<sup>g</sup> Paul Scherrer Institute, 5232 Villigen, Switzerland

<sup>h</sup> Climate and Environmental Physics, Physics Institute and Oeschger Centre for Climate Change Research, University of Bern, 3012 Bern, Switzerland

<sup>i</sup> Southern Oregon University, Biology Department, Ashland, OR 97520, USA

### ARTICLE INFO

#### Article history:

Received 5 June 2015

Received in revised form

11 December 2015

Accepted 15 December 2015

Available online xxx

#### Keywords:

Northeastern Yakutia

Stable isotopes in tree-ring width

Permafrost

Thaw depth

Water source

Climate

### ABSTRACT

Tree-ring width and stable isotopic composition are widely used for the reconstruction of environmental conditions. Eco-physiological models simulating  $\delta^{13}\text{C}$  and  $\delta^{18}\text{O}$  provide tools to constrain the interpretation of measured tree-ring variations and their relationships to environmental variables. Here, we apply biochemical models of photosynthesis and a model of stomatal conductance to simulate the intra-annual dynamics of  $\delta^{13}\text{C}$  values in photo assimilates and tree-rings. We use these models to investigate the physiological responses of larch trees growing on permafrost to variability in precipitation and permafrost depth associated with regional temperature and precipitation changes. Tree-ring width,  $\delta^{13}\text{C}$  and  $\delta^{18}\text{O}$  in wood and cellulose were measured in larch (*Larix cajanderi* Mayr.) samples from northeastern Yakutia (69°N, 148°E) for the period from 1945 to 2004 and used for comparisons with modeled  $\delta^{13}\text{C}$  and  $\delta^{18}\text{O}$  data.

Mechanistic models that quantify physical and biochemical fractionation processes leading to oxygen isotope variation in organic matter are used to identify source water for trees growing on permafrost in Siberia. These models allowed us to investigate the influence of a variety of climatic factors on Siberian forest ecosystem water relations that impact isotope fractionation.

Based on  $\delta^{13}\text{C}$  and  $\delta^{18}\text{O}$  in tree wood and cellulose measurements as well as outputs from different eco-physiological models, we assume that larch trees from northeastern Yakutia can have limited access to the additional thawed permafrost water during dry summer periods.

© 2015 Istituto Italiano di Dendrochronologia. All rights reserved.

### 1. Introduction

Boreal forests are the largest ecosystems on the earth (Apps et al., 2006). Trees growing on permafrost in these ecosystems are sensitive to climate change, e.g., temperature increase, reduc-

tion in precipitations, thawing permafrost (Sugimoto et al., 2002; ACIA, 2004). Because of temperature increases, vapour pressure deficit (VPD) will likely increase as well resulting in increased evapotranspiration, which is especially impactful on tree's water relations. Measurements have shown no change in precipitation inputs, which may enhance drought stress in situations where enhanced water loss is not compensated by greater moisture inputs (Pachauri et al., 2014). Trees from the Boreal zone respond to both the timing and magnitude of changes in soil moisture and soil temperature, as well as permafrost thickness and its distribution, which itself is directly affected by snow and vegetation cover, soil

\* Corresponding author at: University of Bern, Institute of Geological Sciences, Dendrolab.ch, 3012 Bern, Switzerland.

E-mail addresses: [olga.churakova@geo.unibe.ch](mailto:olga.churakova@geo.unibe.ch), [olga.sidorova@bluewin.ch](mailto:olga.sidorova@bluewin.ch) (O.V. Churakova (Sidorova)).

texture and geothermal heat flux (Cable et al., 2013; Boike et al., 2013). The fate of trees growing on permafrost undergoing climatic and environmental changes is of great interest, because of the important role permafrost plays in these ecosystems and the large amounts of carbon stored in these soils (Cable et al., 2013). Boreal forests are particularly at risk with rising temperatures due to consistently low precipitation inputs (200–250 mm per year) (Sidorova et al., 2010; Boike et al., 2013). A number of studies have reported a pronounced deepening of seasonal permafrost thaw in Western Siberia (Moskalenko, 2001; Melnikov, 2004; Pavlov, 2004; Fyodorov-Davydov et al., 2009). Fyodorov-Davydov et al. (2009) investigated the spatial and temporal trends in the active soil layer (ASL) in North Yakutia, which is the top layer of soil with high activity of microbial processes and which thaws during the summer and freezes again during the autumn. No long-term measurements of active soil layer depth are known for northeastern Yakutia. Previous studies (Vaganov et al., 1998; Naurzbaev et al., 2002; Hughes et al., 1999) have shown the importance of June–July temperatures for larch tree growth in the Siberian north. Precipitation and permafrost melt water are particularly crucial for trees growing in regions with severe temperature limitations (Sidorova et al., 2007, 2010). Due to low temperatures in Siberian north, water loss is not yet as large as observed in European forest ecosystems (Saurer et al., 2014). However, with a continued increase in temperature (Sidorova et al., 2010), drought stress may increase accordingly.

Subarctic forests are remote from population centers, which, on one hand, allow the study of natural processes controlling these systems without direct anthropogenic impacts (i.e., management, introduction of exotic species). The disadvantage is that there are very few weather stations. There is only one weather station near Chokurdach, which is located 200 km away from our study site and unfortunately contains gaps in weather observations making it difficult to obtain appropriate meteorological data. Gridded large scale climate data ( $5^\circ \times 5^\circ$  latitude/longitude) can help to fill in the gaps in the missing climate data from the local weather stations. Using the gridded temperature and precipitation data is an important source of information that can be used to quantify climate reconstructions during the last decade and further back in time (first half of 20th century). For example, based on tree-ring width chronologies we extracted temperature signals using both, local weather, and gridded data (<http://climexp.knmi.nl>) back in time (>100 years) (Sidorova et al., 2010). However, changes in precipitation for these tree-line sites, where temperature is such an important factor, are difficult to reconstruct.

Stable carbon ( $\delta^{13}\text{C}$ ) and oxygen ( $\delta^{18}\text{O}$ ) isotopes capture not only temperature signals but also record important information about moisture and precipitation changes. Climatic parameters like temperature, water availability, air humidity and the impact of changes in ambient  $\text{CO}_2$  on photosynthetic  $\text{CO}_2$  assimilation and water balance are reflected in the isotopic carbon and oxygen ratios of plant organic matter, potentially providing an isotopic fingerprint in the wood of tree rings. The analysis of tree physiological properties using carbon isotope ratios is particularly useful when combined with a photosynthesis model that considers the influence of meteorological conditions on plant functions, such as stomatal conductance and the substomatal vs. the ambient  $\text{CO}_2$  concentrations ( $c_i/c_a$  ratio) (Farquhar et al., 1989; Arneeth et al., 2002; Vaganov et al., 2006).

Oxygen isotopes in organic matter are modified by variation in the isotopic composition of source water, which is closely related to that of precipitation and soil water (though modified by evaporation at the soil surface). The  $\delta^{18}\text{O}$  of meteoric water is directly related to cloud/atmosphere air temperatures (Dansgaard, 1964) as well as evaporation and condensation processes in the global water cycle. Input waters are modified (enrichment in  $^{18}\text{O}$ ) in the leaf during transpiration, which is imprinted on photosynthates

and cellulose through biochemical fractionation and exchange processes.

In Siberia, the inter-annual variability of winter precipitation  $\delta^{18}\text{O}$  is closely related to temperature variability and the North Atlantic Oscillation, while the variability of summer  $\delta^{18}\text{O}$  appears to be dominated by regional-scale processes involving evaporation and convection (Butzin et al., 2014). Therefore,  $\delta^{18}\text{O}$  values of tree rings reflect, as a first approximation, average ambient temperatures and humidity. Progress has been made in understanding the fractionation processes, which an  $\text{H}_2^{18}\text{O}$ -molecule undergoes from soil water to cellulose in tree rings (Craig and Gordon, 1965; Dongmann et al., 1974; Farquhar and Lloyd 1993; Roden et al., 2000). These models have been validated with experimental data from deciduous and coniferous tree species. Roden et al. (2000) developed a model, which takes environmental inputs as well as the isotopic exchange between cellulose and xylem water into account. The isotopic composition of leaf water can be theoretically estimated using the Craig–Gordon model (Craig and Gordon, 1965). The maximal enrichment according to the Craig–Gordon model is only reached at the evaporating surfaces. Bulk leaf water is less enriched than Craig–Gordon estimates because xylem water moves into the leaf via transpirational flux, which is modified by the back diffusion of enriched water from the evaporating surfaces as described by the Péclet effect (Farquhar and Lloyd, 1993).

In our study, we hypothesize that Siberian larch trees (*Larix cajanderi* Mayr.) from northeastern Yakutia growing on continuous permafrost will profit from using thawed permafrost water as an additional water source to survive periods of drought stress. An alternative hypothesis is that trees may go into decline because thawed permafrost water will still be too cold to be taken up by roots.

To test our hypotheses we applied mechanistic  $\delta^{13}\text{C}$ ,  $\delta^{18}\text{O}$  eco-physiological models and measured  $\delta^{13}\text{C}$ ,  $\delta^{18}\text{O}$  in wood and cellulose of larch trees (i) to reveal the interaction between trees and precipitation changes as well as changes of active soil layers due to thawing of permafrost under temperature and  $\text{CO}_2$  changes in the atmosphere; (ii) to reveal the most important climatic variables that influence intra-annual dynamics of  $\delta^{13}\text{C}$  and  $\delta^{18}\text{O}$  in tree-ring wood and cellulose formation; and (iii) to describe the water-use of trees in permafrost ecosystems and the impact of permafrost thaw depth.

## 2. Material and methods

### 2.1. Study site and tree-ring width chronologies

Sampling of larch (*L. cajanderi* Mayr) was performed in northeastern Yakutia ( $69^\circ\text{N}$ ,  $148^\circ\text{E}$ ), near the At-Khaya Mountains at the upper timberline in the forest tundra of the central Indigirka lowland at 250–350 m a.s.l. Crown density of larch forest tundra is low 0.5. The peat-gley and shallow gley soils prevail in the tundra zone as well as gley frozen soils that dominate under sparse taiga forests in southern part of the province. The lower part of the soil profile is covered by continuous low-temperature permafrost that is 500–650 m. thick and has a temperature range of  $-10^\circ\text{C}$ – $-12^\circ\text{C}$  (Fyodorov-Davydov et al., 2009). Surface soil moisture has decreased during June–August in Central Yakutia (Sugimoto et al., 2002). The vegetative period is short and can vary between 50 and 90 days. The average January temperature is  $-34.5^\circ\text{C}$ , and mean July air temperature is  $+9.6^\circ\text{C}$  obtained from the Chokurdach weather station ( $70^\circ30'\text{N}$  and  $148^\circ08'\text{E}$ ) for the period from 1945 to 2004. The highest monthly mean soil temperature for the tundra zone that is covered by continuous permafrost is recorded in August ( $+4.1^\circ\text{C}$ ) from a sensor depth of 0.06 m, while year to year variability in the mean soil temperatures from June to October

were in a range of  $\pm 3.5^\circ\text{C}$ . However, greater variations in soil temperatures (up to  $10^\circ\text{C}$ ) were recorded in November and December (Boike et al., 2013).

For our  $\delta^{13}\text{C}$  and  $\delta^{18}\text{O}$  modeling, we used daily temperature and precipitation data from the Chokurdach weather station for the period from 1948 to 2004. Model output is problematic if based on short-term observations or where many years of data are missing. Gaps in the meteorological data were filled using the CRU TS 3.10 data (New et al., 1999). These complete meteorological data sets were used in the LPX-Bern (Spahni et al., 2013) and ORCHIDEE (Krinner et al., 2005) models (see next sections) for the period from 1901 to 2004. Especially for regions covered by permafrost over the Holocene, the model would use the wrong starting conditions, if it was established with more modern, i.e., warmer, meteorological data.

Using ARSTAN software with options of negative exponential or linear regression curves we built tree-ring width index chronology based on cross-dated tree-ring width (TRW) samples from 143 larch trees (Sidorova and Naurzbaev, 2002; Hughes et al., 1999). TRW,  $\delta^{13}\text{C}$  and  $\delta^{18}\text{O}$  chronologies in wood and cellulose for the study site were constructed based on four discs of larch samples, analyzed separately for each tree with highly significant inter tree correlations for TRW ( $r=0.89$ ,  $P<0.05$ );  $\delta^{13}\text{C}$  ( $r=0.87$ ;  $P<0.05$ ) and  $\delta^{18}\text{O}$  ( $r=0.73$ ;  $P<0.05$ ) for the period from 1880 to 2004 (Sidorova et al., 2007).

## 2.2. Mechanistic eco-physiological models

### 2.2.1. ORCHIDEE model

We used the global mechanistic biogeochemical ORCHIDEE model described in Krinner et al. (2005). The model simulates the exchanges of energy, water and carbon dioxide within the soil–vegetation–atmosphere continuum, temperature, relative humidity, sunshine duration at a half-hourly time step. Input variables, which we used for ORCHIDEE model include: precipitation, humidity, temperature, downward short wave radiation, downward long wave radiation, wind speed, pressure, and atmospheric  $\text{CO}_2$  concentration. The ORCHIDEE model takes only standard heat transfer by diffusion into account. The soil type is an input parameter and was defined as a mix between different possible soil types. In our case, a sandy loam soil 85% sand, 10% loam and 5% clay. The soil pH was set to 6. The model was run with a 2-bucket soil depth, with a total of 2 m-depth. For roots, their density at a given depth is described with an exponential function (exponential decrease of the root density with the depth).

The ORCHIDEE model was run for the period from 1901 to 2004 to simulate annual tree-growth and the stable carbon and oxygen isotopic composition of cellulose. Water input at the soil surface has three origins: rainfall, snow melt, and surface deposition (dew and frost). Water can leave the soil reservoir through transpiration, soil surface evaporation, surface runoff and drainage. Drought stress is calculated as a function of the soil water content weighted by the exponential root profile. The water stress function affects transpiration through the modulation of stomatal conductance and is adapted for needle species like conifers.

### 2.2.2. The LPX-Bern model

To understand processes that may affect plant growth at this permafrost site, such as the interaction with precipitation, freezing and thawing of soil layers, we applied the Land surface Processes and eXchanges (LPX-Bern 1.0) model developed at the University of Bern (Spahni et al., 2013; Stocker et al., 2013). The LPX-Bern model (LPX hereafter) is an improved version of the Lund–Potsdam–Jena (LPJ) dynamic global vegetation model (Sitch et al., 2003; Gerten et al., 2004). LPX simulates water, carbon and nitrogen (N) fluxes between the terrestrial biosphere (soil and vegetation) and the

atmosphere at a daily time step. The model simulates tree growth for an average forest stand age of tree plant functional types (PFTs) competing for light, water, and nutrients (N availability) constrained by bioclimatic temperature limits and atmospheric  $\text{CO}_2$ . In addition to the standard LPJ model, LPX simulates explicit soil heat diffusion, soil water freezing and thawing, and permafrost conditions (Wania et al., 2009), which are particularly applicable to our system.

Permafrost simulation in LPX uses 8 types of mineral soils (Wania et al., 2009). The biggest impact for heat transfer is the separation into mineral soils (7 types) and organic soil (1 peat land soil type) due to the difference in porosity and thus water storage capacity. In this study we use a generic mineral soil type ('Medium texture') (Wania et al., 2009). All other parameters were used as in the published version of the model, here most importantly for photosynthesis (Sitch et al., 2003) and permafrost (Wania et al., 2009). The model is calibrated globally for various soil surfaces, vegetation types and ecosystems. It is a process-based model on simple principles of physics, geography, biology and biogeochemistry. The model was evaluated against observations and tested for the sensitivity of the key outputs (for more details see Wania et al., 2009).

The permafrost module within LPX has been compared to active layer thickness at 20 sites from the Circumpolar Active Layer Monitoring Network, where of 8 sites are in Russia and 3 of these sites in Yakutia (Wania et al., 2009). Modelled seasonal soil temperatures have been compared to measurements at four stations in the circumpolar region (Wania et al., 2009). We did not calibrate LPX for the study site, but we tested inter-annual variability of thaw depth with data from a nearby site (Fyodorov-Davydov et al., 2009), where it agrees well.

The presence of permafrost affects rooting depth and water stress, which modifies plant transpiration through changes in stomatal conductance. From calculated stomatal conductance and net photosynthesis rates LPX simulates intrinsic water use efficiency and  $^{13}\text{C}$  of assimilated carbon (Saurer et al., 2014). In order to catch "weather effects" on  $\delta^{13}\text{C}$  in LPX, the total monthly precipitation in the model is distributed randomly on a prescribed number of rainy days per month. For the distribution we use a stochastic model as a Markov chain of the first order, where the probability of rain on a given day depends on the status of the previous day (Richardson, 1981; Srikanthan and McMahon, 1985). Yet, LPX model does not take into account heat transfer with precipitation. LPX uses repeated starting climate conditions of the period 1901–1931 and constant  $\text{CO}_2$  and N deposition of 1901. With these conditions LPX run over 1500 years into equilibrium at 1901. From there a transient simulation was started with variable forcing's over the period 1901–2004.

### 2.2.3. Simulating tree-ring width

We utilized the same four cross-dated tree-ring width (TRW) chronologies from northeastern Yakutia, which were also used for stable carbon and oxygen isotope measurements as TRW inputs for all models. Most global carbon land surface models (e.g., LPX) describe above and below ground mean ecosystem carbon reservoirs. These models allocate net primary production (NPP, resulting from photosynthesis minus autotrophic respiration) to different reservoirs but there is no accounting for individual tree growth. Comparisons with TRW are restricted to quantifying the relationship between observed intra-annual variations (IAV) of TRW with the IAV of the NPP allocated each year to sapwood.

Recently, the ORCHIDEE model has been largely improved with the addition of a new "Forest Management" module and the mode of management was set to "Self-thinning" referred to as ORCHIDEE-FM (Bellassen et al., 2010) to simulate growth of individual trees of a forest stand using realistic allometric rules to partition NPP

between leaves, trunk, branches and roots. The mean woody NPP of the stand calculated by ORCHIDEE is distributed unevenly across the different diameter classes following the observed rule that smaller trees have less NPP than dominant bigger trees (Deleuze et al., 2004).

The outputs of ORCHIDEE-FM are time-series of tree-ring widths (in mm) for the different diameter classes. The parameters of diameter classes were simulated for trees similar to real cored trees and can thus be directly compared with the measured time-series. Note that the first 10 years of tree growth, which are highly affected by “age effects” during juvenile stages (Cook et al., 1990), are not taken into consideration, as these effects are difficult to model.

#### 2.2.4. Models describing carbon isotopic signature in tree rings

The Benkova and Shashkin (2003) (BS-model) was developed based on the photosynthesis model for simulating NPP variation. The BS-model is driven by daily climatic data and based on the calculations by the daily time step of photosynthesis and respiration rates, water balance in the soil, and variation of stomatal conductance as a function of soil moisture and relative humidity (Benkova and Shashkin, 2003; Vaganov et al., 2006). The daily  $\delta^{13}\text{C}$  was calculated according to Farquhar et al. (1989). The tree-ring isotopic composition was calculated as a weighted mean of daily  $\delta^{13}\text{C}$  where the weights are the percent daily NPP of the total for the growth period.

In the BS-model daily NPP was integrated for the whole growing season for each year and then an index relative to the mean value was calculated with the goal to compare observed ring width chronologies with index chronologies. Soil moisture and soil temperature are important parameters for the permafrost zone and were included in the model (Vaganov et al., 2006).

The ORCHIDEE, LPX and BS models use the standard equations for photosynthetic carbon isotope discrimination ( $\Delta^{13}\text{C}$ , preferential uptake of the lighter  $^{12}\text{CO}_2$  isotope) in  $\text{C}_3$  species, according to Farquhar et al. (1989):

$$\Delta^{13}\text{C} = a + (b - a) \times \frac{c_i}{c_a} \quad (1),$$

where  $a$  (4.4‰) is the kinetic discrimination associated with diffusion between free air and the substomatal cavity,  $b$  (27‰) describes the kinetic enzyme fractionation during carboxylation of  $\text{CO}_2$  via Rubisco,  $c_i$  is the leaf internal  $\text{CO}_2$  concentration, simulated by BS, ORCHIDEE, and LPX (Benkova and Shashkin, 2003; Saurer et al., 2014) and  $c_a$  is the atmospheric  $\text{CO}_2$  concentration.

The carbon isotope composition of newly formed photosynthate is calculated half-hourly (ORCHIDEE) or daily (LPX) according to:

$$(2), \delta^{13}\text{C}_{\text{photosynthesis}} = \frac{(\delta^{13}\text{C}_{\text{atmosphere}} - \Delta^{13}\text{C})}{(1 + \Delta^{13}\text{C})}$$

The output  $\delta^{13}\text{C}$  of the ORCHIDEE, LPX and  $\delta^{13}\text{C}$  models were corrected according to the Suess effect (Francey et al., 1999). The ORCHIDEE model accounted for the timing of transport of newly formed photosynthates from the leaves to the trunk, as well as mixing with remobilized carbon compounds from previous year's stored carbohydrates, while this is not the case for the LPX and BS models. In the LPX model this mixing of remobilized carbon is not considered and simulated  $\delta^{13}\text{C}$  reflects the isotopic signature of annually allocated biomass carbon. In the LPX model photosynthesis and  $\delta^{13}\text{C}$  of gross primary production (GPP) is simulated daily. It is assumed that  $\delta^{13}\text{C}$  of daily NPP is identical to  $\delta^{13}\text{C}$  of daily GPP. Monthly and annual  $\delta^{13}\text{C}$  averages are then weighted by daily and monthly NPP respectively, where  $\text{NPP} > 0$ .

#### 2.2.5. Models describing oxygen isotopic signature in tree rings

We used a modified version of the terrestrial biosphere ORCHIDEE model and the Roden–Lin–Ehleringer (Roden et al., 2000) mechanistic model (RLE) to simulate  $\delta^{18}\text{O}$  variation in cellu-

lose time series. The model calculates the isotopic composition of leaf water at the site of evaporation according to Crag and Gordon (1965) and Dongmann et al. (1974).

$$\delta^{18}\text{O}_{\text{evap}} = \delta^{18}\text{O}_{\text{source}} + \varepsilon_e + \varepsilon_k + (\delta^{18}\text{O}_{\text{vapor}} - \delta^{18}\text{O}_{\text{source}} - \varepsilon_k) \times \frac{e_a}{e_i} \quad (3),$$

where  $\delta^{18}\text{O}_{\text{evap}}$  is the isotope ratio at the site of evaporation,  $\delta^{18}\text{O}_{\text{source}}$  is the water taken up by the roots and can be a mixture of older soil water and recent precipitation,  $\varepsilon_e$  is the equilibrium fractionation due to the phase change from liquid water to vapour,  $\varepsilon_k$  is the kinetic fractionation due to diffusion of vapour into unsaturated air,  $\delta^{18}\text{O}_{\text{vapor}}$  is the isotopic composition of atmospheric water vapour, and  $e_a/e_i$  the ratio of external to internal water vapour pressures respectively (Craig and Gordon, 1965; Dongmann et al., 1974).

To include leaf boundary layer considerations and the diffusion through stomata for modeling leaf water the expanded Craig and Gordon model was applied Eq. (4) (Farquhar et al., 1989; Flanagan et al., 1991; Roden et al., 2000).

$$R_{\text{wl}} = \alpha \times \left[ \alpha_k R_{\text{ws}} \left( \frac{e_i - e_s}{e_i} \right) + \alpha_{\text{kb}} R_{\text{wx}} \left( \frac{e_s - e_a}{e_i} \right) + R_a \left( \frac{e_a}{e_i} \right) \right] \quad (4),$$

where  $R$ ,  $\text{wl}$ ,  $a$ ,  $i$ ,  $s$ ,  $\text{wx}$ —refer to the  $^{16}\text{O}/^{18}\text{O}$  isotope ratio, leaf water, bulk air, sub-stomatal partial pressure for water vapor, partial pressure for water vapor at the leaf surface and xylem water (source water), respectively.  $\alpha$  liquid–vapour equilibrium fractionation factor and varies with temperature (Majoube, 1971).  $\alpha_k$ —the kinetic fractionation is associated with diffusion in air;  $\alpha_{\text{kb}}$ —the kinetic fractionation is associated with diffusion through the boundary layer and is calculated by increasing  $\alpha_k$  to the 2/3 power ( $^{16}\text{O}/^{18}\text{O} = 1.0189$ ) (see Flanagan et al., 1991; Roden et al., 2000).

The isotopic composition of cellulose is predicted as function of both the isotopic ratio of the substrate sucrose and of the medium water at the site of cellulose synthesis be it leaf, root, or xylem cells as part of the tree-ring (Saurer et al., 1997; Roden et al., 2000). The  $\delta^{18}\text{O}$  in tree-ring cellulose ( $\delta^{18}\text{O}_{\text{cx}}$ ) is calculated as:

$$\delta^{18}\text{O}_{\text{cx}} = f_0 \times (\delta^{18}\text{O}_{\text{wx}} + \varepsilon_0) + (1 - f_0) \times (\delta^{18}\text{O}_{\text{wl}} + \varepsilon_0) \quad (5),$$

where  $f_0$  is the fraction of exchange with medium water ( $\delta^{18}\text{O}_{\text{wx}}$ ) and estimated to be 0.42 for oxygen from the best fit relationship derived from controlled experiments (see Roden and Ehleringer, 2000). The subscripts  $\text{cx}$  is xylem cellulose,  $\text{wx}$  is xylem water,  $\text{wl}$  is leaf water at the site of sucrose synthesis. The parameter  $\varepsilon_0$  is the biochemical fractionation associated with water carbonyl interactions (27‰) (Sternberg and DeNiro, 1983; Luo and Sternberg, 1992).

The RLE model was used to find the best fit of tree-ring cellulose  $\delta^{18}\text{O}$  observations by modifying water source  $\delta^{18}\text{O}$  values potentially used by larch trees. Input parameters such as maximum air temperature and relative humidity were obtained from the Chokurdach weather station for the period from 1948 to 2004. In general,  $\delta^{18}\text{O}$  of the atmospheric humidity is more depleted in both deuterium and  $\delta^{18}\text{O}$  than source water, but it can vary seasonally in deuterium by as much as 60‰ as storm fronts progress (see White and Gedzelman, 1984). Since no values are available for our study site, we assumed that atmospheric vapor  $\delta^{18}\text{O}$  was 11‰ lighter than water extracted from soil and roots from our Siberian sites. As a first approximation, we employed ranges between  $-28$  and  $-25$ ‰ for changes in snow/melt water and  $-6$ ‰ to  $-11$ ‰ for rain water (Kurita et al., 2005; Prokushkin, personal communication).

Measured Barometric pressure varies with elevation and weather patterns. The value is assumed to be simply an elevation function, in our case based on the latitude 350 m a.s.l. the

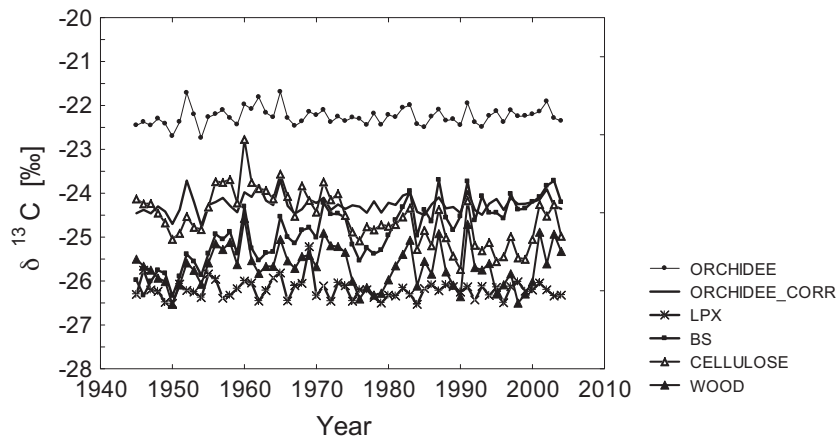


**Fig. 1.**  $\delta^{13}\text{C}$  in cellulose simulated by ORCHIDEE, LPX and BS-models and  $\delta^{13}\text{C}$  in wood simulated by BS-model vs. measured  $\delta^{13}\text{C}$  chronology for the period from 1945 to 2004. The ORCHIDEE\_CORR line shows the output of the ORCHIDEE model after a 2‰ correction for post-photosynthetic fractionation.

barometric pressure was 95 kPa (see Pearcy et al., 1989). Values for stomatal conductance could range widely but we used  $0.3 \text{ mol m}^{-2} \text{ s}^{-1}$ , assuming a low stomatal conductance for larch needles from a cold region. Using Eqs. (3) and (4) we modeled leaf water and based on Eq. (5) cellulose.

The ORCHIDEE-18O version accounts for fractionation during evaporation at the soil surface (as well as at the surface of intercepted water) and within leaves during transpiration. It is based on a modified version of the Craig and Gordon (1965) equation that describes the preferential evaporation of the lighter isotope ( $^{16}\text{O}$  vs.  $^{18}\text{O}$ ) of a free water body at steady state. Note that we do not account for fractionation associated with diffusion in the vapor phase in the soil (Melayah et al., 1996). The main effect that controls tree-ring  $\delta^{18}\text{O}$  corresponds to the enrichment in  $^{18}\text{O}$  within the leaves (where transpiration occurs) with respect to the isotopic composition of soil water that is itself primarily controlled by the isotopic composition of precipitation water and thus by climate.

### 3. Results and discussion

#### 3.1. $\delta^{13}\text{C}$ measured and modelled data

$\delta^{13}\text{C}$  of larch wood and cellulose chronologies were measured annually for each tree separately and corrected for the Suess effect using the  $\delta^{13}\text{C}$  of atmospheric  $\text{CO}_2$  (Francey et al., 1999) for the period from 1945 to 2004 (Sidorova et al., 2007). The range of offset between individual  $\delta^{13}\text{C}$  cellulose chronologies varies from 0.01 to 1.9‰, while  $\delta^{13}\text{C}$  wood chronologies from 0.03 to 2‰ (Sidorova et al., 2007). Measured  $\delta^{13}\text{C}$  values for wood and cellulose chronologies were compared with  $\delta^{13}\text{C}$  chronologies simulations derived from the ORCHIDEE, LPX and BS models to reveal how well they capture temperature and precipitation signals recorded in tree-rings in order to improve the interpretation of tree ring  $\delta^{13}\text{C}$  climate relationships back in time. The measured  $\delta^{13}\text{C}$  in wood and cellulose agreed well with the BS and ORCHIDEE models in terms of intra-annual variability (Fig. 1, Table 1).

We found a substantial offset between the modeled  $\delta^{13}\text{C}$  using ORCHIDEE as compared to both the BS estimated and measured  $\delta^{13}\text{C}$  values in wood and cellulose chronologies. However, even with the high offset of approximately 4‰ between  $\delta^{13}\text{C}$  modeled by ORCHIDEE and measured  $\delta^{13}\text{C}$  chronologies they were still correlated (Table 1). Using the ORCHIDEE  $\delta^{13}\text{C}$  model, Danis et al. (2012) found similar results (biases), arguing that the offset relates to strong anthropogenic and/or canopy effects, which could modify the mean  $\delta^{13}\text{C}$  of atmospheric  $\text{CO}_2$  compared to the background values used in the model. We suggest, that more plau-

sibly, the ORCHIDEE model may not take into account the difference between photosynthates and cellulose  $\delta^{13}\text{C}$  due to additional fractionation events during post-photosynthetic biochemical processes (e.g., Schmidt and Gleixner, 1998; Gessler et al., 2014). Measured values between recent assimilates and cellulose show a difference between 1.8‰ to 2.2‰, where the recent assimilates have a more negative  $\delta^{13}\text{C}$  value than cellulose, a similar difference was found between bulk wood and cellulose. Therefore, we included the resulting isotopic modification into variable  $\Delta^{13}\text{C}_{\text{C-p}}$  post-photosynthetic fractionation events. In the literature,  $\Delta^{13}\text{C}_{\text{C,p}}$  ranges between  $-2 \pm 2\%$  (Boutton, 1996) and  $+2\%$  (Verheyden, 2005).

Based on the Verheyden (2005) assumption we included a 2‰ correction to initial ORCHIDEE\_CORR model output. Using this approach the offset of the ORCHIDEE simulation was significantly smaller compared to the measured carbon isotope chronologies for wood and cellulose (Fig. 1).

Modelled LPX  $\delta^{13}\text{C}$  did not produce positive excursions of about 1‰ as observed in wood and cellulose  $\delta^{13}\text{C}$  values. LPX produced rather constant  $\delta^{13}\text{C}$  values, around  $-26\%$ . While the low range  $\delta^{13}\text{C}$  values in wood were similar, the highest values were about 1‰ more positive,  $\sim -25\%$ .  $\delta^{13}\text{C}$  of cellulose and the output from the BS model show a similarly large variability, but with an average offset ca. 0.31‰ for the period from 1945 to 2004. The reason the LPX model does not produce these more positive values is because simulated plants are not water stressed, as the model simulates sufficient available soil water from precipitation, snow and thawing. The model is entirely driven by temperature, precipitation, cloud cover and number of wet days per month. Relative humidity or VPD forcing are not prescribed in the LPX model. For example, the LPX model is not responsive to extremely low humidity. The LPX model has accurately predicted  $\delta^{13}\text{C}$  values and reconstructed water use efficiencies from trees across European climatic regions (Saurer et al., 2014), but seems to miss an important process at our cold and dry permafrost site. In a sensitivity analysis with the LPX model we tested whether soil freezing and permafrost formation could affect tree growth and  $^{13}\text{C}$  discrimination. In this simulation, freezing was deactivated and the soil water remained liquid, but cool during winter. The effect on  $\delta^{13}\text{C}$  is nearly unchanged compared to the standard simulation, which includes freezing.

This could be explained by the fact that tree growth below  $+5^\circ\text{C}$  is very small or practically zero (Körner 2015). Therefore, the isotope signal, which could be impacted by a frozen soil would not be stored in tree rings, because there is practically no growth. The correlation with measured  $\delta^{13}\text{C}$  wood ( $r=0.38$ ;  $P<0.05$ ) and cellulose ( $r=0.30$ ;  $P<0.05$ ) chronologies based on LPX sensitive simulation

**Table 1**  
Pearson correlation coefficients between BS, LPX, ORCHIDEE, RLE models and measured  $\delta^{13}\text{C}$  and  $\delta^{18}\text{O}$  in wood and cellulose data sets.

Model	Parameter	BS $\delta^{13}\text{C}$	LPX $\delta^{13}\text{C}$	ORCHIDEE $\delta^{13}\text{C}$	RLE $\delta^{18}\text{O}$	ORCHIDEE $\delta^{18}\text{O}$	Wood $\delta^{13}\text{C}$	Wood $\delta^{18}\text{O}$	Cellulose $\delta^{13}\text{C}$	Cellulose $\delta^{18}\text{O}$
BS	$\delta^{13}\text{C}$	1.00								
LPX	$\delta^{13}\text{C}$	0.25	1.00							
ORCHIDEE	$\delta^{13}\text{C}$	0.37*	0.27	1.00						
RLE	$\delta^{18}\text{O}$	0.30*	0.28	0.37*	1.00					
ORCHIDEE	$\delta^{18}\text{O}$	-0.04	0.32*	0.48*	0.39*	1.00				
Wood	$\delta^{13}\text{C}$	0.74*	0.38*	0.52*	0.28	0.39*	1.00			
Wood	$\delta^{18}\text{O}$	0.16	0.39*	0.29	0.78*	0.28	0.29	1.00		
Cellulose	$\delta^{13}\text{C}$	0.32*	0.30*	0.51*	0.16	0.30	0.78*	0.23	1.00	
Cellulose	$\delta^{18}\text{O}$	0.29	0.35*	0.41*	0.92*	0.41*	0.32*	0.84*	0.23	1.00

\* Significant value;  $P < 0.05$  for the common period for all data sets from 1948 to 2004.

remains similar to standard  $\delta^{13}\text{C}$  wood ( $r = 0.35$ ;  $P < 0.05$ ) and cellulose ( $r = 0.38$ ;  $P < 0.05$ ) data, compared to the results of the BS or ORCHIDEE models. Because  $\delta^{13}\text{C}$  was nearly identical in the standard and sensitivity simulations, we conclude that variation in relative humidity and VPD at northeastern Yakutia seems to be dominated by atmospheric conditions (top-down) and not by soil-vegetation interactions (bottom-up). This differs from what has been generally observed in simulations with European ecosystems (Saurer et al., 2014). However, if we look at the simulated thaw depth in LPX (Fig. 2), we find a correlation with measured  $\delta^{13}\text{C}$  in wood ( $r = 0.56$ ;  $P < 0.05$ ) (Fig. 1). The positive correlation (deeper thawing related to more positive  $\delta^{13}\text{C}$ ) indicates that water from deeper layers may not be available for larch because increasing  $\delta^{13}\text{C}$  indicates stomatal closure and drought stress rather than increased water supply. Using LPX, the simulated thaw depth was significantly correlated with VPD during summer months June–August, where the highest correlation was found with July VPD ( $r = 0.42$ ;  $P < 0.05$ ) (Fig. 2). Positive correlations of modeled permafrost thaw depth with June–August VPD indicate a water deficit at the study site. Recently available new short-term measurements of permafrost thaw depth for northern Yakutia (Fyodorov-Davydov et al., 2009) show similar patterns as found with our LPX simulations (Fig. 2). It has to be noted LPX does not take into account heat transfer with precipitation. So this indeed may affect the simulation of soil temperature in wet years at this cold and remote site.

Sugimoto et al. (2002) showed that larch (*Larix gmelinii* Rupr.) trees could use thaw melt water from the soil layers up to 1.2–1.4 m during dry summers in Spasskaya Pad near Yakutsk city. However, the authors concluded, if thaw occurred too deeply, it would be difficult for roots to take up thawed water, as a consequence larch trees could be seriously damaged by water deficits during summer drought. On the other hand, Cable et al. (2013) reported that thawing permafrost can also result in a deeper active soil layer, which increased the potential plant rooting volume.

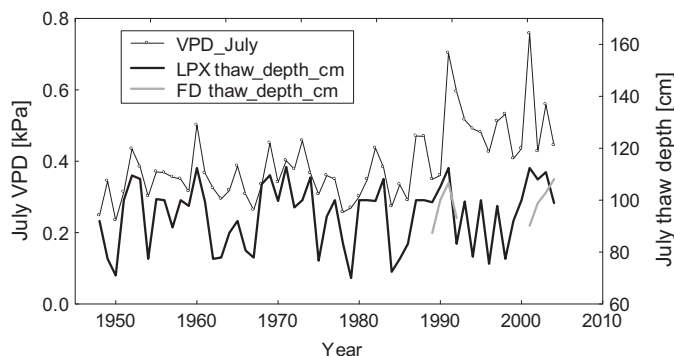


**Fig. 2.** Thaw depth is simulated by the LPX model in centimetres (cm) for July vs. July VPD data, obtained from the Chokurdach weather station for the period from 1948 to 2004. The real short-term measurements of permafrost thaw depths from northern Yakutia (FD) (Fyodorov-Davydov et al., 2009) in comparison.

Based on the LPX modeled annual water fraction per year (Fig. 3) there was not much variability in the soil depths  $> 100$  cm. High variability was found for soil depths between 10–20 cm, which correlated significantly with  $\delta^{13}\text{C}$ , measured in wood ( $r = 0.36$ ;  $P < 0.01$ ).

We found significant correlations between modeled water fractions at soil depths of 20–30 cm ( $r = 0.40$ ;  $P < 0.01$ ) and 30–40 cm ( $r = 0.32$ ;  $P < 0.05$ ) with July temperature respectively. These correlations indicate an active soil layer at 20–30 cm, where larch roots could have access to water.

Cable et al. (2013) reported that at their study site in Fairbanks, Alaska, soil temperature at 10 cm depth corresponded with the active organic layer and was, therefore, an important depth for affecting stomatal conductance and transpiration. Similar findings were revealed by Ruess et al. (2006), who found that the bulk of roots occur, at the top 20 cm of soil.

The LPX modeled water fraction at 0–10 and 10–20 cm soil depths correlated with June VPD ( $r = 0.41$ ;  $P < 0.01$  and  $r = 0.51$ ;  $P < 0.01$ ), respectively. The LPX modeled water fraction at 10–20 and 20–30 cm depths significantly correlated with July VPD ( $r = 0.44$ ;  $P < 0.01$ ; and  $r = 0.32$ ;  $P < 0.05$ ), respectively.

Air can become very dry during the summer in northeastern Yakutia.  $\delta^{13}\text{C}$  chronologies indicate that trees were exposed to drought leading to stomatal closure. Increased temperatures at the beginning of the growing season were probably not large enough to melt permafrost so that water uptake by trees was strongly limited. In addition, if there are not enough precipitations at the beginning of the growing season or snow thaw water, then this can exacerbate drought stress for trees.

No significant correlation was detected with August VPD, while negative correlations between LPX modeled water fraction at 10 cm soil depth were found with September VPD, indicating that soil water starts freezing in September. Boike et al. (2013) reported that thaw starts around 15 June and soils begin to freeze again around 29 September for 2004 on Samoylov Island, Lena River Delta ( $72^\circ\text{N}$ ,  $126^\circ\text{E}$ ).

### 3.2. $\delta^{18}\text{O}$ measured and modeled data

Since very little is known about precipitation changes and sources of water in northeastern Yakutia and Northern Siberia in general, we applied the ORCHIDEE and RLE models to test the relationship between modeled and measured wood and cellulose  $\delta^{18}\text{O}$  chronologies (Fig. 4). The range of offset between individual  $\delta^{18}\text{O}$  cellulose chronologies obtained from four larch trees was from 0.01 to 3.4‰, and for  $\delta^{18}\text{O}$  wood was from 0.08 to 3.3‰, for more detail see (Sidorova et al., 2007).

We also modeled potential water sources (Fig. 5), which might be used by larch trees on the Siberian north in the permafrost zone. We found highly significant correlations between our measured  $\delta^{18}\text{O}$  in wood and cellulose as compared to predictions derived from the RLE and ORCHIDEE models (Table 1). However,

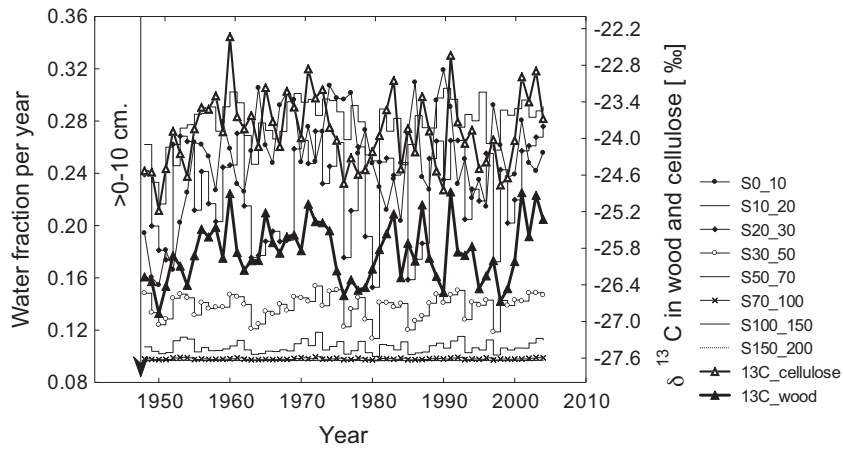


**Fig. 3.** Variation of the LPX simulated annual water fraction per year for different soil depths and  $\delta^{13}\text{C}$  measured in wood (13C.wood), and  $\delta^{13}\text{C}$  in cellulose (13C.cellulose). Soil depths are presented from S0.10 (soil depth from 0 to 10 cm), S10.20 (from 10 to 20 cm), S20–30 (from 20 to 30 cm), S50–70 (from 50 to 70 cm), S70–100 (from 70 to 100 cm), S100–150 (from 100 to 150), S150–200 (from 150 to 200 cm).

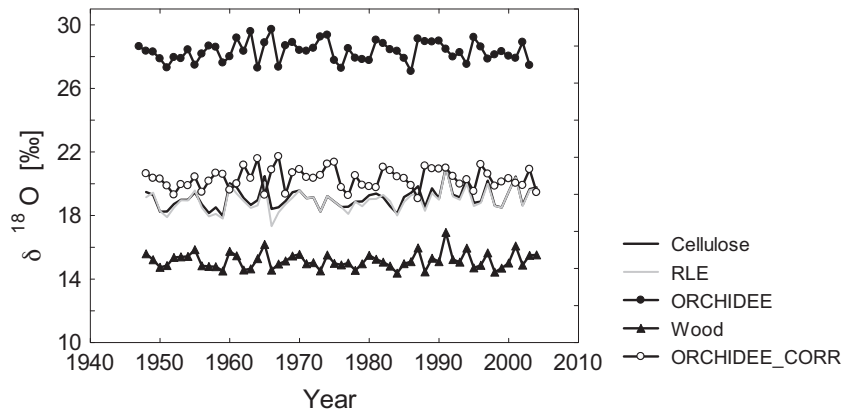


**Fig. 4.** Modeled initial ORCHIDEE and ORCHIDEE.CORR corrected from 8% systematic offset and RLE  $\delta^{18}\text{O}$  chronologies vs. measured  $\delta^{18}\text{O}$  wood and cellulose chronologies.

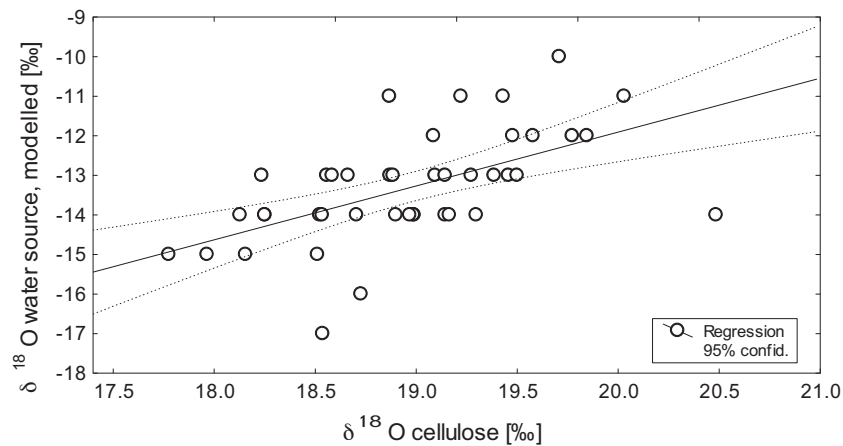


**Fig. 5.** Scatter plot of the modeled RLE  $\delta^{18}\text{O}$  water source vs.  $\delta^{18}\text{O}$  cellulose chronology with the 95% confidence interval.

the ORCHIDEE chronology showed a clear offset by almost 8%. This offset could be explained by errors in the representation of the water storage capacity in the soil at the study site, or rooting depth and thus estimates of source water  $\delta^{18}\text{O}$  were too high. The ORCHIDEE  $\delta^{18}\text{O}$  model may also overestimate the proportion of soil evaporation to total evapotranspiration due to the high-latitude effect (Dansgaard, 1964). This effect is described by water vapor gradients that develop as moisture transits from the tropics to the

poles, which gradually became more and more depleted in  $^{18}\text{O}$ . Such a large offset is a problem and needs to be taken into account for further ORCHIDEE model development. The RLE model showed some agreement with the ORCHIDEE model (Table 1), but showed a much stronger correspondence with the measured values. The regression ( $R^2 = 0.48$ ;  $P < 0.05$ ) between  $\delta^{18}\text{O}$  source water and  $\delta^{18}\text{O}$  cellulose was significant, showing that 50% of the variation is explained by source water variation (Fig. 5). The rest of the

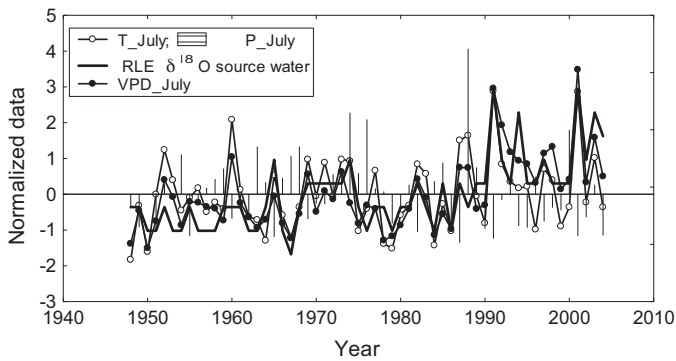


**Fig. 6.** Time series of RLE  $\delta^{18}\text{O}$  modeled water source and Chokurdach weather station data for July temperature (T\_July), precipitation (P\_July) and July VPD for the period from 1948 to 2004. Chronologies are normalized relative to zero.

variation was most likely related to leaf evaporative enrichment in response to VPD and tree physiological parameters in particular stomatal responses to environmental variations (i.e., temperature, ambient humidity, and  $\delta^{18}\text{O}$  of water vapor).

We found significant correlations between RLE modelled  $\delta^{18}\text{O}$  water source and Chokurdach weather station data for July VPD ( $r=0.80$ ;  $P<0.01$ ), as well as July temperature ( $r=0.59$ ;  $P<0.01$ ) and precipitation ( $r=-0.29$ ;  $P<0.03$ ) (Fig. 6).

Normalized data for the average mean July temperature ( $+15.3^\circ\text{C}$ ) and the average July VPD (0.32 kPa) for the period from 1948 to 2004 are presented (Fig. 6). The simulation revealed extreme ( $\geq 2\sigma$ ) July temperature and July VPD during 1960 ( $+20^\circ\text{C}$ ; 0.24 kPa), 1991 ( $+21.8^\circ\text{C}$ ; 0.70 kPa) and 2001 ( $+21.7^\circ\text{C}$ ; 0.76 kPa), for the study period. During the same years,  $\delta^{13}\text{C}$  in wood and cellulose, TRW, and modeled  $\delta^{13}\text{C}$  and  $\delta^{18}\text{O}$  data showed similar extremes, with deviations  $\geq 2\sigma$  for the year 1960 for  $\delta^{13}\text{C}$  wood ( $\sigma=2.3$ ),  $\delta^{13}\text{C}$  cellulose ( $\sigma=3$ ), for 1991:  $\delta^{13}\text{C}$  wood ( $\sigma=2.1$ ),  $\delta^{18}\text{O}$  wood ( $\sigma=3.3$ ),  $\delta^{18}\text{O}$  cellulose ( $\sigma=2.7$ ),  $\delta^{18}\text{O}$  RLE ( $\sigma=3.03$ ) and for 2001 for  $\delta^{18}\text{O}$  RLE ( $\sigma=2.1$ ). TRW measurements as well as BS and LPX models also produced standard deviations  $<2\sigma$ .

Extremely high precipitation ( $4\sigma$ ) was recorded in July 1988 ( $3.8\text{ mm}^{-1}$ ) according to Chokurdach weather station data. Wet July ( $2\sigma$ ) months were also observed in 1974 ( $2.6\text{ mm}^{-1}$ ) and 1976 ( $2.4\text{ mm}^{-1}$ ). Interestingly, only July temperature,  $\delta^{18}\text{O}$  wood and simulated  $\delta^{18}\text{O}$  ORCHIDEE model output showed ( $>1\sigma$ ) deviations from the average for the year of 1988.

Saurer et al. (2015) showed that comparison of wet and dry summers,  $\delta^{18}\text{O}$  soil was 3–4‰ lower in dry years for the permafrost site in Tura ( $64^\circ\text{N}$ ,  $100^\circ\text{E}$ ). The drier summer conditions led to lower  $\delta^{18}\text{O}$  in top soil, indicating more influence of melting permafrost water (or possibly winter/spring water) which apparently influences the upper soil levels when these tend to dry out.

The positive correlations between July VPD and modeled source water  $\delta^{18}\text{O}$  goes along with a reduction of stomatal conductance and a further increase in  $\delta^{18}\text{O}$  enrichment in the source water points to a developing water shortage. The negative correlation with July precipitation is weak and could be explained by the low amount of precipitations at the study site.

Moreover, the LPX modeled water fraction of soil depth is significantly correlated with the RLE  $\delta^{18}\text{O}$  modeled source water with significant correlations up to 100 cm depth, and highest correlations at soil depths of 10–20 cm ( $r=0.38$ ;  $P<0.01$ ) and 20–30 cm ( $r=0.36$ ;  $P<0.05$ ). Based on the LPX model we estimated that soils thawed as deep as 100 cm (Fig. 2) during the period from 1948 to 2004.

Recently, the number of eco-physiological studies in permafrost regions have increased (Boike et al., 2013; Bryukhanova et al., 2015;

Saurer et al., 2015). However, applications of eco-physiological models to tree-ring parameters (TRW,  $\delta^{13}\text{C}$ ,  $\delta^{18}\text{O}$ ) are still rare.

Here we present a novel combined analysis using multiple models that predict  $\delta^{13}\text{C}$  and  $\delta^{18}\text{O}$  variation in tree-rings, which may help to disentangle the impact of important hydro-climatic factors such as the interplay between water source, soil moisture and soil thaw depth influencing tree growth under permafrost conditions. The discrepancies between modeled and measured data are in part due to different parameterizations but also due to the different model designs for different ecosystems (e.g., Saurer et al., 2014). However, each model had its strengths and weaknesses and in their complementarity they represent a powerful tool (Benkova and Shashkin, 2003; Krinner et al., 2005; Spahni et al., 2013; Saurer et al., 2014).

Dynamics of soil moisture and soil temperature appear to be the dominant factors for predicting  $\delta^{13}\text{C}$  variation in the permafrost zone.  $\delta^{13}\text{C}$  values simulated by the ORCHIDEE and BS models for the period from 1948 to 2004 correlated significantly with measured data from wood and cellulose, respectively. Based on simulated thaw depth and the corresponding water fraction as well as stable isotope measurements, we conclude that larch trees from northeastern Yakutia during dry periods (1950-, 1960-, 1990s) most likely have additional access to the soil moisture from thawed permafrost but not below 50–70 cm (Fig. 2). Fyodorov-Davydov et al. (2009) showed that during long-term measurements for tundra, Indigirka Lowland ( $70^\circ33'\text{N}$ ,  $147^\circ26'\text{E}$ ), from 2004 to 2006 active layer thicknesses are varied up to 64–65 cm. LPX modeled water fraction of soil depths indicated that the active soil layer for larch trees was most likely between 20 and 50 cm.

Further simulations of thaw depth and  $\delta^{18}\text{O}$  values, using the RLE model for estimating source water  $\delta^{18}\text{O}$  over time indicates additional water sources. We assume that increased  $\delta^{18}\text{O}$  of source water ( $-24\text{‰}$  to  $-19\text{‰}$ ) from 1948 to 1990 may indicate a possible access of larch trees to additionally thawed permafrost water (Fig. 6). Yet, the question remains whether larch trees (*L. cajanderi* Mayr) from northeastern Yakutia can utilize this water. Furthermore, simulations with the RLE model indicate that July rain water was the most utilized source for the period from 1945 to 2004. RLE simulations also indicate that source water enrichment (in  $^{18}\text{O}$ ) increased over time, possibly because of an increase in temperature resulting in higher evapotranspiration due to higher VPD and drier conditions for these trees.

#### 4. Conclusion

1. Our results based on  $\delta^{13}\text{C}$  and  $\delta^{18}\text{O}$  measurements, and based on data from eco-physiological models suggest that larch trees from northeastern Yakutia during the dry periods have additional access to soil moisture from thawed permafrost.

2. We presented a novel combined analysis using multiple models that predict  $\delta^{13}\text{C}$  and  $\delta^{18}\text{O}$  variation in tree-rings, which may help to disentangle the impact of important hydro-climatic factors such as the interplay between water source, soil moisture and soil thaw depth influencing tree growth under permafrost conditions. Permafrost plays a crucial role in the soil's capability, whether precipitation or snowmelt water can be stored in the soils or is lost as run-off, depending on permafrost depth.

3. Extending applications of tree-ring parameters (tree-ring width, stable carbon and oxygen isotopes) inferred from trees growing on the Subarctic to mechanistic eco-physiological models will improve our knowledge about interactions between thawing permafrost and tree productivity under global warming scenarios. The application of improved models for forest vegetation in recent and past times will lead to more realistic evaluations and reliable predictions of ongoing climatic change and help to make predic-

tions of possible changes not only on regional but also on global scales.

## Acknowledgements

This work was supported by Marie Curie Fellowships (IIF EU-ISOTREC 235122; RP 909122) awarded to Olga Sidorova and ELVECS FP7 Era.Net project; The Russian Science Foundation – RSF (project #14-14-00219) for the simulation approaches. We thank Alexander Kirilyanov, Paolo Cherubini and two anonymous Reviewers for the valuable comments reviewing our manuscript.

## References

- ACIA, 2004. *Impacts of a warming arctic*. In: Arctic Climate Impact Assessment. ACIA Overview report. Cambridge University Press, pp. 140.
- Arneeth, A., Lloyd, J., Santruckova, H., Bird, M., et al., 2002. Response of central Siberian Scots pine to soil water deficit and long-term trends in atmospheric CO<sub>2</sub> concentration. *Global Biogeochem. Cycles* 16 (1), <http://dx.doi.org/10.1029/2000GB001374>.
- Apps, M.J., Shvidenko A. Z., Vaganov E. A., 2006. Boreal Forests and the Environment: A Foreword, Mitigation and Adaptation Strategies for Global Change, 11(1) 1–4.
- Bellassen, V., Le Maire, G., Dhôte, J.F., Ciais, P., Viovy, N., 2010. Modelling forest management within a global vegetation model—Part 1: model structure and general behaviour. *Ecol. Modell.* 221, 2458–2474.
- Benkova, A.V., Shashkin, A.V., 2003. The photosynthesis of pine and larch and its relation with radial increment. *Lesovedenie (Russ. J. Sci.)* 5, 1–6.
- Boike, J., Kattenstroth, B., Abramova, K., et al., 2013. Baseline characteristics of climate, permafrost and land cover from a new permafrost observatory in the Lena Rive Delta, Siberia (1998–2011). *Biogeosciences* 10, 2105–2128.
- Bryukhanova M.V., Fonti P., Kirilyanov A.V., Siegwolf R.T.W., Saurer M., Pocheby N.P., Churakova O.V. (Sidorova), Prokushkin, A.S. (2015) The response of (<sup>13</sup>C, <sup>18</sup>O) and cell anatomy of *Larix gmelinii* tree rings to differing soil active layer depths *Dendrochronologia*, 34: 51–59.
- Butzin, M., Werner, M., Masson-Delmotte, V., Risi, C., Frankenberg, C., Gribanov, K., Jouzel, J., Zakharov, V.I., 2014. Variations of oxygen-18 in West Siberian precipitation during the last 50 years. *Atmos. Chem. Phys.* 14, 5853–5869.
- Cable, J.M., Ogle, K., Bolton, R.W., et al., 2013. Permafrost thaw affects boreal deciduous plant transpiration through increased soil water, deeper thaw and warmer soil. *Ecohydrology*, 10.1002/eco.1423.
- Cook, E., Briffa Shiyatov, K.S., Mazepa, V., 1990. *Tree-ring standardization and growth trend estimation*. In: Cook, E.R., LA, Kairiukstis (Eds.), *Methods of Dendrochronology: Applications in the Environmental Sciences*, pp. 104–123.
- Craig H., Gordon L.I., 1965. Deuterium and oxygen 18 variations in the ocean and marine atmosphere. In *Proc. Stable Isotopes in Oceanographic Studies and Paleotemperatures*, Spoleto, Italy. Edited by Tongiogi, E., Lishi F., Pisa. 9–130.
- Dansgaard, W., 1964. *Stable isotopes in precipitation*. *Tellus* 16, 436–468.
- Deleuze, C., Pain, O., Dhôte, J.F., Hervé, J.C., 2004. A flexible radial increment model for individual trees in pure even-aged stands. *Ann. For. Sci.* 61, 327–335.
- Dongmann, G., Nürnberg, H.W., Förstel, H., Wagener, K., 1974. On the enrichment of H<sub>2</sub><sup>18</sup>O in the leaves of transpiring plants. *Radiat. Environ. Biophys.* 11, 41–52.
- Farquhar, G., Lloyd, J., 1993. Carbon and oxygen isotope effects in the exchange of carbon dioxide between terrestrial plants and the atmosphere. In Ehleringer, J.R., Hall, A.E.
- Farquhar, G.D., Hubick, K.T., Condon, A.G., Richards, R.A., 1989. Carbon isotope fractionation and plant water-use efficiency. In: Rundel, J.R., Ehleringer, K.A. (Eds.), *Stable Isotopes in Ecological Research*. Springer-Verlag, New York, pp. 21–40.
- Fyodorov-Davydov, D.G., Kholodov, V.E., Kraev, G.N., Sorokovikov, V.A., Davydov, S.P., Merekalova, A.A., 2009. Seasonal thaw of soils in the North Yakutian ecosystems. In: V International Conference on Cryopedology Diversity of forest affected soils and their role in ecosystems, At Ulan-Ude, Buryatia, Russia, September 14–20.
- Flanagan, L.B., Comstock, J.P., Ehleringer, J.R., 1991. Comparison of modeled and observed environmental influences on the stable oxygen and hydrogen isotope composition of leaf water in *Phaseolus vulgaris* L. *Plant Physiol.* 96, 588–596.
- Francey, R.J., Allison, C.E., Etheridge, D.M., et al., 1999. A 1000-year high-precision record of (<sup>13</sup>C in atmospheric CO<sub>2</sub>). *Tellus B* 51, 170–193.
- Gerten, D., Schaphoff, S., Haberlandt, U., Lucht, W., Sitch, S., 2004. Terrestrial vegetation and water balance—hydrological evaluation of a dynamic global vegetation model. *J. Hydrol.* 286, 249–270.
- Gessler, A., Ferrio, J.P., Hommel, R., Treydte, K., Werner, R.A., Monson, R.K., 2014. *Tree Physiol.* 34 (8), 796–818.
- Hughes, M.K., Vaganov, E.A., Shiyatov, S.G., Touchan, R., Funkhouser, G., 1999. Twentieth-century summer warmth in northern Yakutia in a 600-year context. *Holocene* 9 (5), 603–608.
- Körner, C., 2015. Paradigm shift in plant growth control. *Curr. Opin. Plant Biol.* 25, 107–114.
- Krinner, G., Viovy, N., de Noblet-Ducoudre, N., Ogee, J., Polcher, J., Friedlingstein, P., Ciais, P., Sitch, S., Prentice, I.C., 2005. A dynamic global vegetation model for studies of the coupled atmosphere–biosphere system. *Glob. Biogeochem. Cycles*, <http://dx.doi.org/10.1029/2003GB002199>, B002199.
- Luo, Y.H., Sternberg, L., 1992. Hydrogen and oxygen isotope fractionation during heterotrophic cellulose synthesis. *J. Exp. Bot.* 43, 47–50.
- Majoube, M., 1971. Fractionnement en oxygène-18 et en deutérium entre l'eau et sa vapeur. *J. Chim. Phys.* 58, 1423–1436.
- New, M., Hulme, M., Jones, P., 1999. Representing twentieth-century space-time climate variability. Part I: development of a 1961–90 mean monthly terrestrial climatology. *J. Climate* 12, 829–856.
- Melayah, A., Brückler, L., Bariac, T., 1996. Modeling the transport of water stable isotopes in unsaturated soils under natural conditions 1. *Theory. Water Resour. Res.* 32, 1043–1397, <http://dx.doi.org/10.1029/96WR00674>.
- Naurzbaev, M.M., Vaganov, E.A., Sidorova, O.V., Schweingruber, F.H., 2002. Summer temperatures in eastern Taimyr inferred from a 2427-year late-Holocene tree-ring chronology and earlier floating series. *The Holocene* 12 (6), 727–736.
- Pachauri, R.K., Meyer, L.A., et al., 2014. In: Pachauri, R.K., Meyer, L.A. (Eds.), *IPCC 2014. Climate Change 2014: Synthesis Report Contribution of Working Groups I, II and III to the Fifth Assessment Report of the Intergovernmental Panel on Climate Change*. IPCC, Geneva, Switzerland, p. 151.
- Richardson, C.W., 1981. Stochastic simulation of daily precipitation, temperature, and solar radiation. *Water Resour. Res.* 17 (1), 182–190.
- Roden, J.S., Ehleringer, J.R., 2000. Hydrogen and oxygen isotope ratios of tree-ring cellulose for riparian trees grown long-term under hydroponically controlled environments. *Oecologia* 121, 467–477.
- Roden, J.S., Lin, G., Ehleringer, J.R., 2000. A mechanistic model for interpretation of hydrogen and oxygen isotopic ratios in tree-ring cellulose. *Geochim. Cosmochim. Acta* 64, 21–35.
- Saurer, M., Aellen, K., Siegwolf, R., 1997. Correlating <sup>13</sup>C and <sup>18</sup>O in cellulose of trees. *Plant Cell Environ.* 20, 1543–1550.
- Saurer, M., Spahni, R., Frank, D.C., et al., 2014. Spatial variability and temporal trends in water-use efficiency of European forests. *Global Change Biol.* 20, 3700–3712, <http://dx.doi.org/10.1111/gcb.12717>.
- Schmidt, H.L., Gleixner, G., 1998. Carbon isotope effects on key reactions in plant metabolism and <sup>13</sup>C-patterns in natural compounds. In: *Stable Isotopes: Integration in Biological, Ecological and Geochemical Processes* (ed. H. Griffiths), pp. 13–26. BIOS, Oxford.
- Saurer, M., Kirilyanov, A.V., Prokushkin, A.S., Rinne, K.T., Siegwolf, R.T.W., 2015. The impact of an inverse climate–isotope relationship in soil water on the oxygen-isotope composition of *Larix gmelinii* in Siberia. *New Phytol.*, <http://dx.doi.org/10.1111/nph.13759>.
- Sidorova, O.V., Siegwolf, R., Saurer, M.M., Naurzbaev, M.M., Vaganov, E.A., 2007. Isotopic composition (<sup>δ13</sup>C, <sup>δ18</sup>O) in Siberian tree-ring chronology. *Geophys Res. Biogeosci.* 113, G02019.
- Sidorova, O.V., Siegwolf, R.T.W., Saurer, M.M., Naurzbaev, M.M., Shashkin, A.V., Vaganov, E.A., 2010. Spatial patterns of climatic changes in the Eurasian north reflected in Siberian larch tree-ring parameters and stable isotopes. *Global Change Biol.* 16, 1003–1018.
- Sidorova, O.V., Naurzbaev, M.M., 2002. Response of *Larix cajanderi* to climatic changes at the upper timberline and flood-plane terrace from Indigirka River valley. *Lesovedenie* 2, 73–75 (In Russian).
- Sitch, S., et al., 2003. Evaluation of ecosystem dynamics, plant geography and terrestrial carbon cycling in the LPJ dynamic global vegetation model. *Global Change Biol.* 9, 161–185.
- Spahni, R., Joos, F., Stocker, B.D., Steinacher, M., Yu, Z.C., 2013. Transient simulations of the carbon and nitrogen dynamics in northern peatlands: from the Last Glacial Maximum to the 21st century. *Clim. Past* 9, 1287–1308.
- Srikanthan R., McMahon T.A., 1985. Stochastic generation of rainfall and evaporation data. *Aust. Water Resource. Couns. Teach. Pap.* 84, 301 pp, AGPS, Canberra, ACT, Australia.
- Sternberg Ld. S., DeNiro, M.J., 1983. Biogeochemical implications of the isotopic equilibrium fractionation factor between the oxygen atoms of acetone and water. *Geochim. Cosmochim. Acta* 47, 2271–2274.
- Stocker, B.D., et al., 2013. Multiple greenhouse-gas feedbacks from the land biosphere under future climate change scenarios. *Nat. Clim. Change* 3, 666–672.
- Sugimoto, A., Yanagisawa, N., Fujita, N., Maximov, T.C., 2002. Importance of permafrost as a source of water for plants in east Siberian taiga. *Ecol. Res.* 17 (4), 493–503.
- Vaganov, E.A., Hughes, M.K., Kirilyanov<sup>1</sup>, A.V., Schweingruber, F.H., Silkin, P.P., 1998. Reduced sensitivity of recent tree-growth to temperature at high northern latitudes. *Nature* 391, 678–682.
- Vaganov, E.A., Hughes, M.K., Shashkin, A.V., 2006. *Growth Dynamics of Conifer Tree Rings: Images of Past and Future Environments*. Springer, pp. 353 p.
- Wania, R., Ross, I., Prentice, I.C., 2009. Integrating peatlands and permafrost into a dynamic global vegetation model: 1. Evaluation and sensitivity of physical land surface processes. *Global Biogeochem. Cycle* 23, <http://dx.doi.org/10.1029/2008gb003412>.
- White, J.W.C., Gedzelman, S.D., 1984. The isotopic composition of atmospheric water vapor and the concurrent meteorological conditions. *J. Geophys. Res.* 89, 4937–4939.